Pneumatically Attachable Flexible Rails for Track-Guided Ultrasound Scanning in Robotic-Assisted Partial Nephrectomy—A Preliminary Design Study

Agostino Stilli ⓘ, Emmanouil Dimitrakakis ⓘ, Claudia D'Ettorre ⓘ, Maxine Tran ⓘ, and Danail Stoyanov ⓘ, *Member, IEEE*

Abstract—Robotic-assisted partial nephrectomy is a surgical operation in which part of a kidney is removed typically because of the presence of a mass. Pre-operative and intraoperative imaging techniques are used to identify and outline the target mass, thus the margins of the resection area on the kidney surface. Drop-in ultrasound probes are used to acquire intraoperative images: the probe is inserted through a trocar port, grasped with a robotic-assisted laparoscopic gripper and swiped on the kidney surface. Multiple swipes are performed to define the resection area. This is marked swipe by swipe using an electrocautery tool. During this procedure the probe often requires repositioning because of slippage from the target organ surface. Furthermore, the localization can be inaccurate when the target mass is in locations particularly hard to reach, and thus kidney repositioning could be required. A highly skilled surgeon is typically required to successfully perform this pre-operatory procedure. We propose a novel approach for the navigation of drop-in ultrasound probes: the use of pneumatically attachable flexible rails to enable swift, effortless, and accurate track-guided scanning of the kidney. The proposed system attaches on the kidney side surface with the use of a series of bio-inspired vacuum suckers. In this letter, the design of the proposed system and its use in robotic-assisted partial nephrectomy are presented for the first time.

Index Terms—Medical robots and systems, soft robot applications, soft robot materials and design, soft sensors and actuators, surgical robotics, laparoscopy.

I. INTRODUCTION

ROBOTIC-ASSISTED Partial Nephrectomy (RAPN) is a surgical procedure in which part of a kidney is removed. Typically, this procedure is performed because of the presence of a tumour. RAPN is the second most common robotic assisted surgical procedure worldwide after prostatectomy, with similar number of cases to abdominal hysterectomy [1]. The advantages of this robotic-assisted procedure are detailed in [2], [3]; in [4] it is argued that RAPN can be used in place of open surgery or total nephrectomy in some complex renal tumour cases. The RAPN procedure is thoroughly described in [5]. Methods used for the identification of the tumour include pre-operative Computer Tomography (CT) scans [6], Magnetic Resonance (MR) imaging [7] and intraoperative Ultrasound (US) scans [8].

The use of drop-in US probes for RAPN procedures is widely recognized as the golden standard for the intra-operative detection and margins outlining of the mass targeted. In [9] the authors show that the use of US drop-in probes guided by robotic laparoscopic tools rather than standard laparoscopic tools is beneficial for the surgeon as it significantly increases the dexterity, hence, the field of view of the system. Typically, the probe is inserted through a standard trocar port and the surgeon grasps it with a gripper, picking up the probe from a dedicated slot. The slot is generally designed to match the EndoWrist Prograsp Forceps gripper of the daVinci Surgical System, (Intuitive Surgical Inc., Sunnyvale, CA, US). Once the probe is paired with the gripper, the surgeon can navigate to the target organ to perform the swiping sequence: multiple swipes with the US probe are performed on the kidney surface in order to localise the tumour. Section by section the resection area is outlined and marked with an electrocautery tool. The additional degrees of freedom provided by the dexterous wrist of the robotic-assisted laparoscopic tool navigating the probe in comparison with the standard laparoscopic scenario ease the swiping process, nonetheless, this procedure is still challenging. The US probe often requires repositioning because of slippage from the target organ surface. Furthermore, the localisation can be inaccurate when tumours are in locations particularly hard to reach, e.g., in the back part of the kidney. In such cases, kidney repositioning could be required: rigid
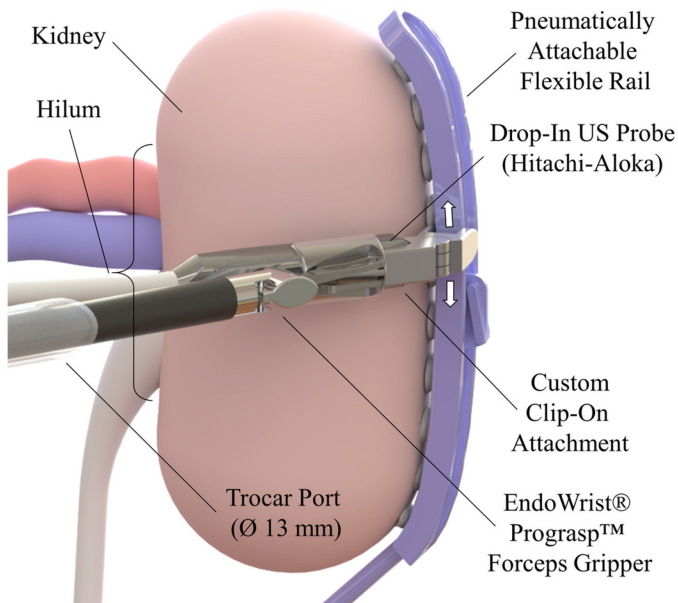
Fig. 1. Pneumatically attachable flexible rails: overview of the system when used to guide a drop-in US probe for tumour margins outlining in RAPN procedures.
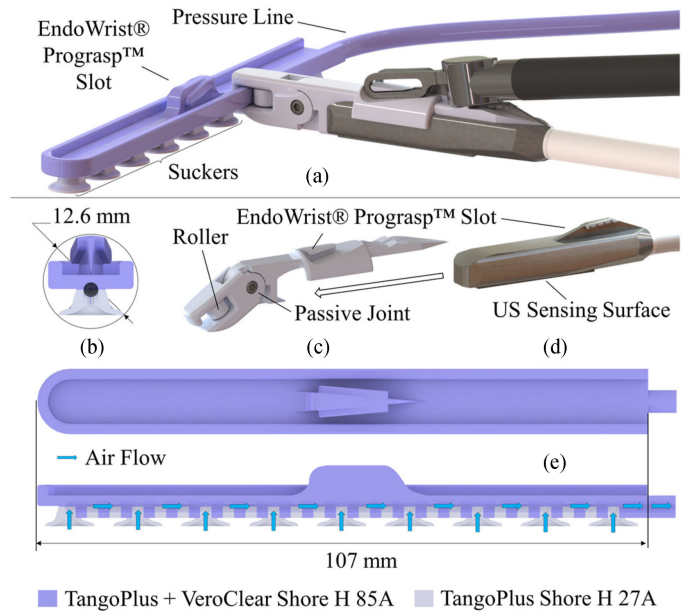

Fig. 2. Overview of the main components of the proposed system: (a) detail of the pairing between the EndoWrist Prograsp Forceps gripper, the custom clip-on attachment (shown detached in (c)), the drop-in US probe Hitachi-Aloka (shown detached in (d)) and the PAF rail. Details of the structure of the PAF rail is shown in cross-section view in (b) and in longitudinal section view in (e), where the air flow between the suckers and the inner channel is also shown by the azure arrows). Purple and gray have been used to indicate the material used to build the structure of the PAF rail, indicating respectively the use of the digital material FLX9985-DM (TangoPlus + VeroClear with Shore Hardness 85 A) and FLX930 TangoPlus (Shore Hardness 27 A). This colour code has been used in all the relevant pictures in this work.

laparoscopic tool are used to apply relatively large forces on small portions of delicate and highly vascularised soft tissues, thus increasing the risk of organ perforation and internal bleeding. A study that examines the perforation risk of endoscopic US procedures on various organs can be found in [10]. For these reasons, a highly skilled surgeon and assistant are typically required to successfully perform this pre-operatory procedure [4], [8]. Similar problems exist in many other medical procedures involving the use of drop-in US probes, e.g., prostatectomy.

In this letter we propose a novel approach for the navigation of US probes: the use of Pneumatically Attachable Flexible rails (PAF Rails) to enable swift, effortless, stable and accurate track-guided scanning of the kidney.

The intended use of the proposed device for track-guidance of drop-in US probes during partial nephrectomy is shown in the CAD drawing in Fig. 1. The proposed system is attached on the kidney side's surface by means of a series of bio-inspired suction cups and it is used as a guide on which the surgeon attaches and slides the drop-in US probe. The design of a custom clip-on attachment for the drop-in US probe is also proposed in this letter in order to enable the pairing and the sliding of the probe along the rail.

The main components of the proposed system are shown in detail in Fig. 2 and they include: the PAF rail (cross-section view in (b), top view and longitudinal section view in (e)) and the custom clip-on attachment (c) designed to pair with the drop-in US probe (Hitachi Aloka), shown in (d). The custom clip-on attachment features the same kind of slot connector as the top part of the drop-in US probe, so that once the two are paired, the surgeon can navigate the assembly in the same way she/he would navigate the probe alone. A flexible pressure line supplies the vacuum pressure to the proximal end of the system, as shown in Fig. 2(a). This line connects with a cavity that runs through the entire length of the PAF rail: suckers are arranged

on a protruding line and connected to the cavity by a series of openings, as shown in Fig. 2(e). The distal end of the cavity is sealed. Once vacuum pressure is applied, all the suckers are simultaneously depressurized. As a result, the suckers, hence, the whole system, firmly connects with any adjacent body surface or organ as long as no gaps are left. As shown in Fig. 2(d), along the whole perimeter of the system, excluding the proximal end, a continuous L-section rail is embedded. A customized slot is also embedded to match the shape of an EndoWrist Prograsp Forceps gripper to facilitate the system positioning during the deployment, as shown in Fig. 2(a).

II. MATERIALS AND METHODS

The design and mechanism of the vacuum-actuated suckers of the PAF rails takes inspiration from the morphology of the suckers of octopus tentacles. The structure and the suction mechanisms of the suction cups of octopus tentacles is examined in [11]–[13] for different species of octopuses. In the attempt to replicate one of the most efficient suction mechanisms in nature, researchers worldwide have investigated several designs of vacuum-based suckers for different robotic applications, e.g., [14], where a soft continuum robotic tentacle that replicates the arm muscles of the octopus during a grasp motion is presented, and [15], where a biomimetic replication of an octopus sucker is used for attachment onto both medical and non-medical environments. Not only the octopus but also the remora suckerfish inspired the design of bio-mimetic suction mechanisms like the

3D printed multi-material adhesive disk presented in [16]. The usefulness of bio-inspired suckers in robotics is evident in [17], where the development of an industrial gripper equipped with vacuum suckers is investigated in the context of unstructured manipulation of soft, rigid and semi-rigid objects. The use of vacuum in surgical applications has been also investigated to navigate micro-robotic systems in the abdominal cavity [18].

In [19] the use of vacuum has been investigated for the navigation of a micro-robotic system on the surface of the heart, whereas in [20] a vacuum-based device has been investigated for its stabilisation. The use of vacuum for short- and long-term anchoring of medical devices in surgical procedures has been also investigated in [21] and [22]. Similar actuation systems and attachment mechanisms are also found in non-medical applications such as the system proposed in [23]. Nonetheless, the concept of pneumatically attachable rails, as well as the concept of rail-like systems for track-based navigation of surgical instruments and sensing probes, has never been proposed to date. Given the novelty of the proposed system, a patent application has been filed (United Kingdom Patent Application No. 1808728.8).

The deployment process of the PAF rails and their use with drop-in US probes can be summarized as follows:

1) The system is passed through a standard trocar port and grasped by the gripper slot with the EndoWrist Prograsp Forceps gripper.
2) The mid-point of the sucker line is placed in contact with the mid-point of the lateral surface of the kidney, opposed to the hilum, as shown in Fig. 1.
3) Vacuum pressure is applied to the sucker line, making the system adhere to the kidney surface in its whole length. Any other robotic-assisted tool can be used to apply a small force on those parts of the system not in suction to allow the pneumatic connection.
4) The system is now firmly connected to the kidney and it is released from the gripper.
5) The drop-in US probe (Hitachi-Aloka pictured in Fig. 1 and Fig. 2(d)), paired with the custom clip-on connector and held with the EndoWrist Prograsp Forceps gripper as shown in Fig. 2(a), it is passed through the same trocar port fitting the pressure line connected to the PAF rail.
6) The drop-in US probe paired with the connector is grasped by the dedicated slot and attached to the rail.
7) The drop-in US probe paired with the connector is moved along the rail to perform the swiping sequence, outlining the tumour, hence, the margins of resection.
8) The margins are now defined, and the drop-in US probe removed.
9) The surgeon performs the resection. The PAF rail stays in place until the end of the procedure to ease the organ repositioning during the resection.
10) The resection is completed and the PAF rail removed together with the portion of the kidney containing the targeted mass.

In Fig. 3 the swiping sequence is demonstrated in an ex-vivo experiment on an adult pig kidney using the Prograsp Forceps controlled by a non-clinical user with the generation one da Vinci Surgical Robot (Intuitive Surgical, Sunnyvale, CA).
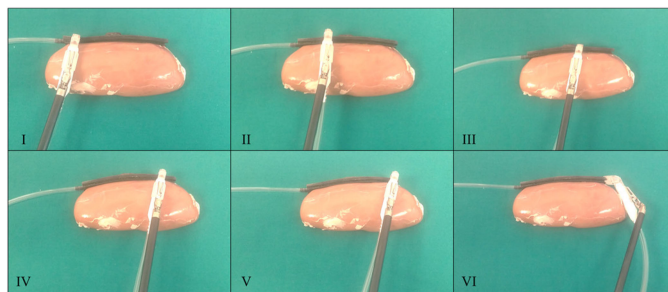

Fig. 3. Swiping sequence: the drop-in US probe (mockup probe 3D printed from CAD model) paired with the custom clip-on connector (3D printed), held by the EndoWrist Prograsp Forceps gripper, attached to the PAF rail and moved along it. Ex-vivo demonstration performed on an adult pig kidney.
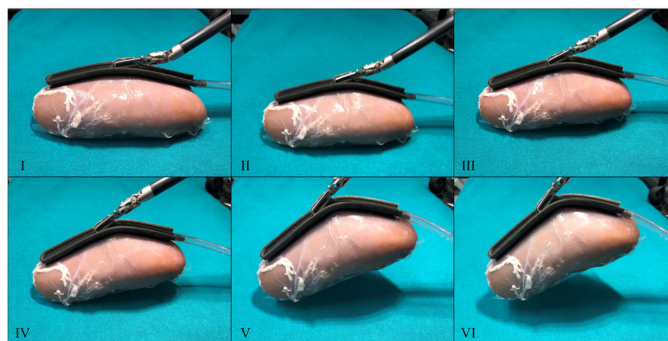

Fig. 4. PAF rail organ repositioning ex-vivo demonstration on adult pig kidney: lifting sequence.

The PAF rails could also be highly beneficial to minimise the risk of perforation when organ repositioning is required.

Once the system is firmly attached on the kidney, the surgeon can use the laparoscopic tool to interact with the PAF rail to mobilise the organ, rather than interacting directly with it. Not only will its flexible structure help to avoid any perforation, but it will also allow distribution of the applied force over a wider surface. Similarly, the proposed system could be used in organ harvesting and transplantation, in place of metallic forceps tools, to grasp the target organs in a safer manner. This use of the proposed system is demonstrated in Fig. 4 where the PAF rail is used to lift the kidney of an adult pig in an ex-vivo experiment.

Another use of the proposed system could be in cardiac surgery procedures, where different methods are employed to compensate for the beating of the heart either completely [24] or partially [25].

The pairing between the PAF rail and the probe (or any other tool based on the same pairing mechanism) ensures a stable interaction even with a pulsating organ.

Given their design, PAF rails can also be used as guide to navigate mini- and micro-robotic systems and to actively constrain the shape of the organ/tissue to which it is attached. Inherently in its design, the proposed system is flexible enough to match the surfaces of the internal organs and cavity walls, but at the same time stiff enough to provide a rail-like structure for robust coupling with any probe/tool sliding along it. To achieve such characteristics, rubber-like materials with low Shore hardness have been used to provide the required compliance to the suckers. Furthermore, materials of higher Shore hardness have been

used to build the walls of the pressure line, in order to prevent it from collapsing once vacuumized. Thus, the use of rubber-like materials of different Shore hardness in the same body element is of paramount importance for the correct functionality of the PAF rails.

At the current stage we have designed and prototyped the proposed system using multi-material multi hardness soft 3D-printing (Model: Objet260 Connex, Stratasys, Eden Prairie, MN, USA). The digital material FLX9985-DM (TangoBlackPlus + VeroClear, Shore Hardness 85 A) has been used for the walls of the internal cavity and the rail. TangoBlackPlus FLX930 material (Shore Hardness 28 A) instead has been used for the suckers.

The designs presented in this work are the results of several qualitative tests conducted at previous design stages with clinical and non-clinical users in our research facilities, as shown in Fig. 3 and Fig. 4.

The aim of this preliminary investigation was the optimization of the shape of the custom clip-on attachment (shown in Fig. 2(c)), of the overall functionality of the proposed system and ultimately of the user experience. Due to space constraints this work does not include further details about these tests.

III. Experimental Results

The aim of the first design study proposed in this letter was to optimize the morphology of the PAF rail in order to guarantee the best possible adherence with the targeted tissue. We would expect that the adhesion will vary with the micro and macro tissue structure as well as the general variability due to the morphology and mass of the organ in question. The whole design of the system was constrained by one parameter: the diameter of the trocar port the system was inserted through to access the abdominal cavity. Being the diameter of the trocar port used to insert the drop-in US probe Hitachi-Aloka 13 mm and being the PAF rail passed through the same or through another port of the same size, the cross section of the proposed system should not exceed such value. As shown in Fig. 2(b), the cross section of the system is inscribed in a 12.6 mm diameter circumference, thus can be easily passed through the trocar port. Standing this constraint, the length of the PAF rail can be customized based on the size of the targeted organ, without affecting its deployability. Another less strong constraint derives from the minimum thickness of the walls that can be printed using the Objet260 Connex, which is 0.8 mm. Lastly, given the Shore hardness of the material used to build the rail-like structure (85 A), a minimum thickness of 1.5 mm for the rail has been deemed necessary to guaranty the robustness of the system and the stability of the connection between the rail edge and the custom clip-on connector.

In order to conduct an extensive optimization study, twelve designs were considered, which are shown in Fig. 5 in perspective and partial longitudinal section view and in partial bottom view. Two main suction cup shapes have been investigated: circular (a–f) and squared (g–l). Three different suction cup densities have been tested: spaced by one (a, b, g, h), adjacent (c, d, i, j) and continuous (e, f, k, l). Two different textures have been considered for the portion of the cup surface in contact with the
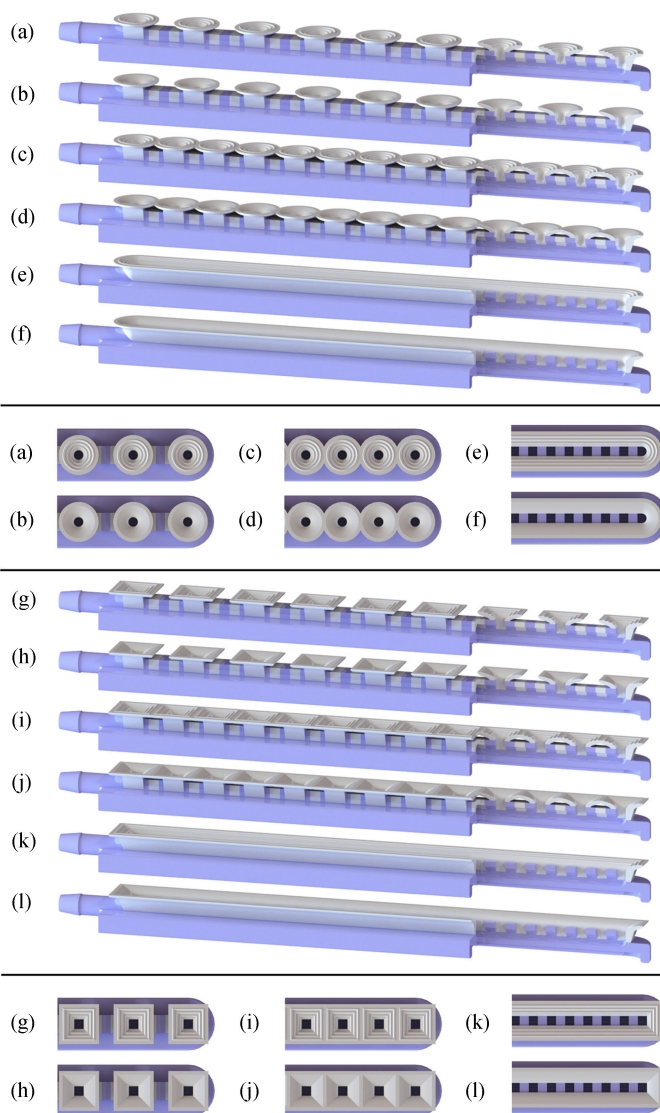

Fig. 5. Samples tested during the proposed design study: circular (a–f) and squared (g–l) suckers were considered and for both designs patterned (a, c, e, g, i, k) and smooth (b, d, f, h, j, l) profiles were evaluated. Different densities of the suckers were tested ranging from spaced by one (a, b, g, h), adjacent (c, d, i, j) and continuous (e, f, k, l).

targeted organ: patterned (a, c, e, g, i, k) and smooth (b, d, f, h, j, l). In order to ease the connection between the PAF rail and the targeted organ a direction of preferential bending for the system has been defined by protruding the structure of the suction cups toward the inner channel, as clearly shown in Fig. 2(e) as well as in the partial longitudinal sections shown for all the samples in Fig. 5. On top of this, soft material inserts have been also added in between cups as also shown in the same figures. In the case of the continuous suction cups (e, f, k, l) given the absence of individual cups, the inserts of soft material were replaced by openings.

As a result, when an external force is applied, all the presented designs, are easier to bend toward the targeted surface, that faces the suction cup(s). Furthermore, when the system is positioned onto an organ and vacuum is applied to the inner channel, the preferential bending direction inherently
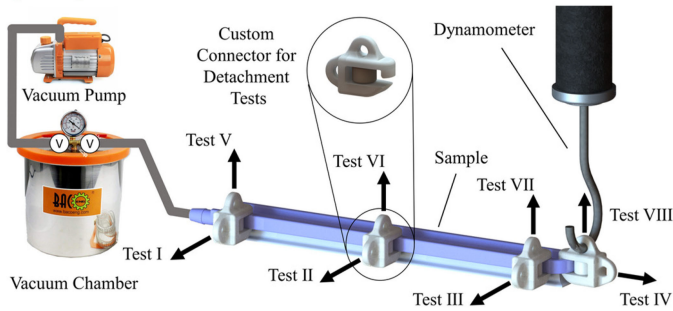
Fig. 6.   Overview of the test rig used for the PAF rail adherence tests including vacuum pump, vacuum chamber (vacuum tank), pressure line (grey), tested sample, custom connector and dynamometer.

embedded in this design can lead to self-adherence of suction cups not yet in suction.

A test rig, which is shown in Fig. 6, was prepared to test the performance of the twelve designs in terms of adherence robustness. A 3 CFM single stage vacuum pump (Bacoeng, Hawthorne, CA) was used to vacuumise a 12-liters vacuum chamber (Bacoeng, Hawthorne, CA) which was used as vacuum tank where the pressure was monitored with the embedded manometer. The vacuum pressure used for all the tests was $P_a = 7.325 \ kPa$. This pressure threshold was selected in order to work in the high-end of the low vacuum range ($P_a = 100$ kPa to 3 kPa [26]), hence, avoiding the use of large, noisy and expensive pumps with considerable vacuuming times, given the intended use of the proposed system in surgical theatres and more generally in healthcare facilities. The possibility of tissue damage was also taken in consideration: qualitative tests were conducted on different tissues with similar properties, size and curvature to the human kidney, like chicken breasts and pig kidneys.

It is important to note that this study did not focus on this particular topic and that a more extensive investigation is needed to understand the effect of the proposed system on highly vascularized organs like the kidneys in order to ensure that no short- nor long-term damage is caused by the suction cups. The chamber was connected with a pressure line (PVC pipe) to the tested PAF rail sample. Eight different tests were performed, testing each of the 12 samples in four different points and in two different directions using a range of spring-based dynamometers (Labworld – Laboratory Equipment – Precision Dynamometer – 1 N, 2 N, 5 N, 10 N, 20 N) to measure the detachment force. The two valves on the chamber were used to put in communication the pump with the chamber and the chamber with the inner channel of the tested sample.

The pneumatic circuit presented in Fig. 6, where the vacuum chamber was used to store vacuum, allowed fine control and monitor the vacuum pressure applied to the system without the need for a closed loop controller with pressure feedback as in the case of a direct connection between the pump and PAF rail. Once the chamber was pressurized and the system was in suction, the pump was switched off and the valve between the pump and the chamber closed. Hence, the pump was not running when the adherence tests took place.

This allowed for a quick drop in the vacuum pressure, without the system going back into suction once disconnection took place, providing consistent results that were not affected by unmodeled pressure dynamics.

During these tests the custom connector shown in Fig. 6 was pulled with the dynamometer until the PAF rails detached. This connector reproduces the shape of the connector designed for the clip-on attachment shown in Fig. 2(c) and these tests aimed at analyzing the behavior of the connector when it comes to interaction forces between the EndoWrist Prograsp Forceps gripper, the attachment and the PAF rail connected to the targeted organ during the intended procedure. The different directions (normal and parallel to surface where the rail is connected) and the different locations where the adherence tests were performed along the rail (proximal, middle, distal and tip) are presented in Fig. 6 and labelled with Roman numbers. This set of tests provided relevant information about the behavior of the system during the user interaction, allowing to test all the directions along which the user can accidentally pull the system causing its detachment. Two set of tests were conducted to assess the performance of the proposed system in diametrically opposite scenarios: when attached on a rigid, flat and smooth surface and on a soft, curved and irregular surface.

For the former scenario a flat smooth sheet of PVC was used. This test provides a good reference for an almost ideal adherence scenario. For the latter instead, a whole chicken breast was used, providing a testing scenario that comes close to the morphology of the organs targeted in the envisioned application. The chicken tissue used during the adherence tests was replaced after every series of four tests (I-IV and V-VIII) to avoid excessive dryness. Thus, given that each test was repeated five times, ten different tissue samples were used. The test order was randomized after each series of tests in order to give more statistical significance to data collected. The chicken tissue was fixed on a wooden board with a system of needles and clamps, ensuring a stable connection with the board. To increase the repeatability of the tests the position of the system on the surface of the chicken tissue was marked with ink for each test series.

To give statistical significance to the collected results each of the eight tests conducted on each of the twelve samples on both rigid and soft material were conducted five times. The force values collected in such manner for all these combinations were then averaged and plotted as bars in the graphs of Figs. 7 to 10. Each bar in these graphs presents the mean value and an error bar on top of it showing the variance of the collected values. Fig. 7 and Fig. 8 show the results for the tests conducted on the smooth rigid surface (PVC) and Fig. 9 and Fig. 10 show the results for the tests conducted on soft organic tissue (chicken breast).

As shown in the graphs of Figs. 7 to 10, despite our best efforts to make the dataset as consistent as possible, some test results are subject to larger variability than others. Among the sources of variability, we should account for system positioning repeatability on the target surface during the tests, especially for the soft tissue cases, resulting in small misalignments between the dynamometer and the custom connector.
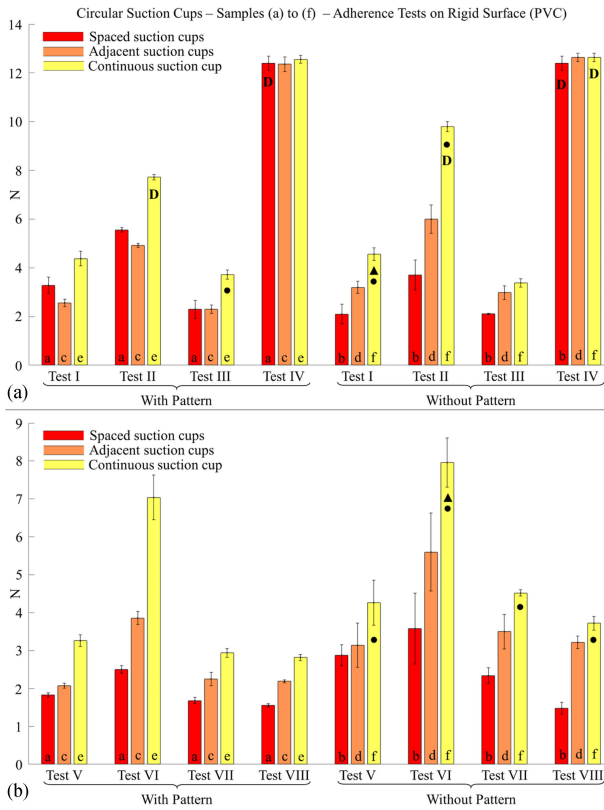
Fig. 7.   Adherence test results for samples (a) to (f) of Fig. 5 (samples name indicated in the bar base) during tests I-VIII performed on rigid smooth surface (PVC). "●" indicates the best performance in a given test for a given design between the version with and without pattern for all the suckers densities considered. "▲" indicates the best overall performance in a given test for all the considered designs (a to l). D indicates that the custom connector for the adherence test has been detached from the PAF rail without the PAF rail being detached from the underlying surface.
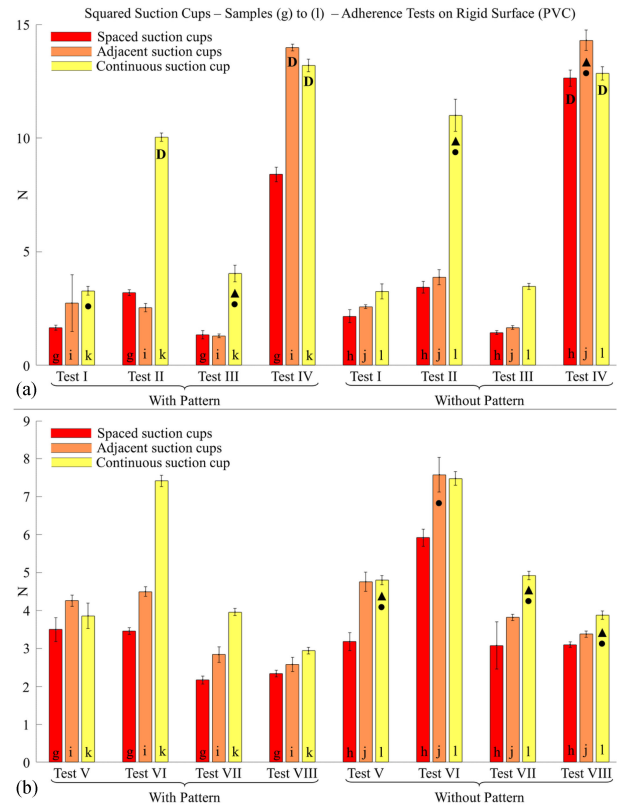
Fig. 8.   Adherence test results for samples (g) to (l) of Fig. 5 (samples name indicated in the bar base) during tests I-VIII performed on rigid smooth surface (PVC). "●" indicates the best performance in a given test for a given design between the version with and without pattern for all the suckers densities considered. "▲" indicates the best overall performance in a given test for all the considered designs (a to l). D indicates that the custom connector for the adherence test has been detached from the PAF rail without the PAF rail being detached from the underlying surface.

The goal of the adherence tests was to choose the best design for the needs of our surgical application, thus to find the best solution in terms of firmness of the connection. In order to select the PAF rail design that performed the best we used as indicator the sum of all the mean detachment force values showed in the graphs of Figs. 7 to 10 of all the eight tests conducted with each sample. This indicator offered us a simple way to compare the overall performance of all the tested systems. The chosen indicator equally weights the performance of the proposed system for all the eight tests considered. This weighting was chosen given the two-fold use of the proposed system i.e., rail to guide the US probe shear stress and interface for organ repositioning. In the former the shear stress is more important for correct performance of the swiping sequence, whereas in the latter the normal stress is more important for stable organ manipulation. In light of this, considering both functions of the same importance, we decided to weight all the test performance equally. Obviously, different applications of the proposed system can be considered, where a function could be of more importance than another, thus a different design can be preferred.

The calculated indicators for all the tested designs for the tests performed on a rigid smooth surface (PVC) are presented in Table I. As shown in Table I, design (f) is the best performing

among the circular designs and (l) is the best performing among the squared designs. It is evident both for the circular and the squared designs, that those with continuous suction cups, (e), (f), (k) and (l), have by far the greatest performance than both the ones with the spaced and the ones with adjacent suction cups. This can be explained with the larger active suction surface that these designs offer, thus the larger force needed to detach them from the surface they are connected to. Based on these results, the design exhibiting the best performance on a rigid surface is (l). A single continuous suction cup without any pattern offers the best possible adherence on a smooth flat surface.

The same indicators calculated for the adherence tests conducted on soft organic tissue (chicken breast) are presented in Table II. The test results on an organic soft tissue followed a similar behavioural pattern with the ones on a rigid surface. Once again, of all the circular designs the two highest performers are the continuous designs (e) and (f). The same applies to the squared designs, were the continuous designs (k) and (l) significantly outperformed their adjacent and space counterparts. Only this time, design (k), namely the patterned squared design with continuous cups, showed the best performance. We believe this being due to the deformability of the tissue surface, which allows the samples with a patterned suction cup to offer a larger
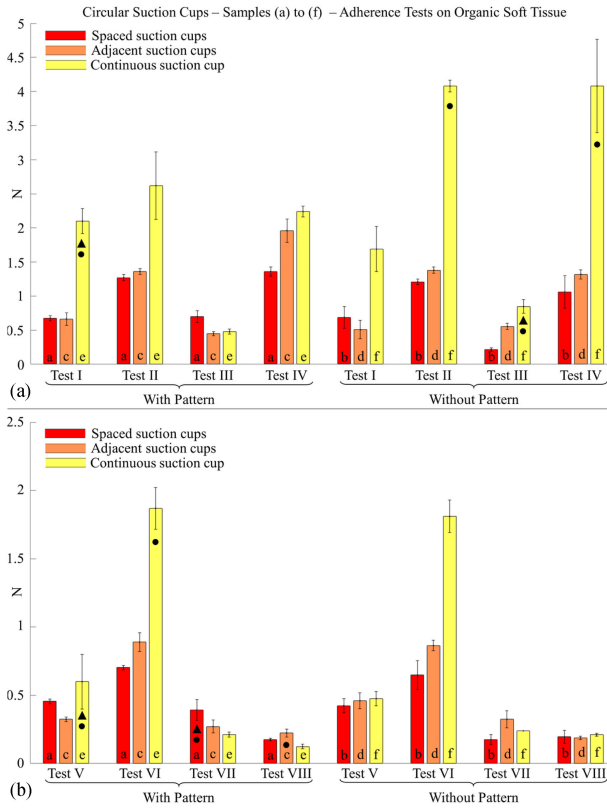
Fig. 9. Adherence test results for samples (a) to (f) of Fig. 5 (samples name indicated in the bar base) during tests I-VIII performed on organic soft tissue (chicken breast). "●" indicates the best performance in a given test for a given design between the version with and without pattern for all the suckers densities considered. "▲" indicates the best overall performance in a given test for all the considered designs (a to l). D indicates that the custom connector for the adherence test has been detached from the PAF rail without the PAF rail being detached from the underlying surface.
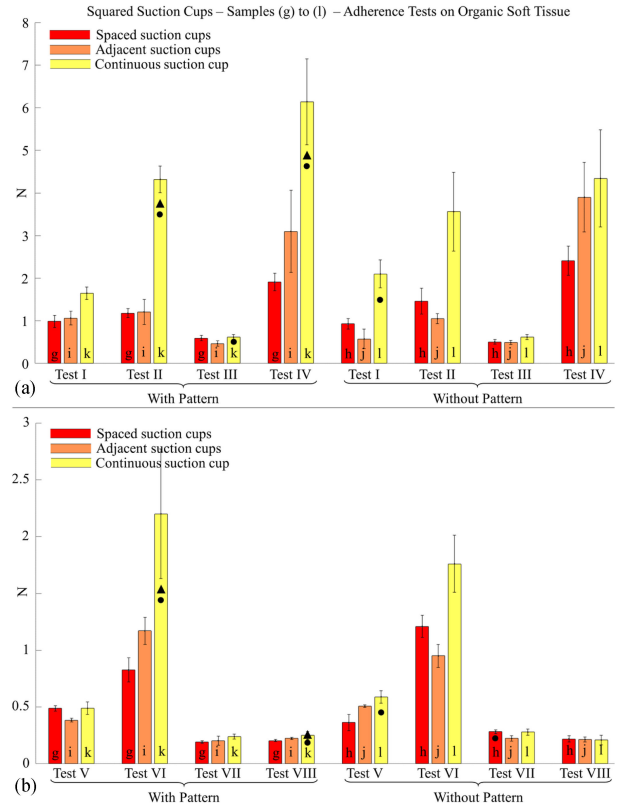

Fig. 10. Adherence test results for samples (g) to (l) of Fig. 5 (samples name indicated in the bar base) during tests I-VIII performed on organic soft tissue (chicken breast). "●" indicates the best performance in a given test for a given design between the version with and without pattern for all the suckers densities considered. "▲" indicates the best overall performance in a given test for all the considered designs (a to l).

TABLE I

PERFORMANCE INDICATORS FOR ALL THE SAMPLES FOR THE ADHERENCE TESTS ON A SMOOTH RIGID SURFACE (PVC). THE COLOUR CODE IS THE SAME USED IN FIGS. 7–10 (RED - SPACED, ORANGE - ADJACENT AND YELLOW - CONTINUOUS SUCTION CUPS)

Sample	Indicator	Sample	Indicator	
(a)	31.1	(b)	30.5	
(c)	32.5	(d)	40.2	Circular
(e)	44.4	(f)	50.8	
(g)	26.0	(h)	34.9	
(i)	34.7	(j)	41.9	Squared
(k)	48.7	(l)	51.6	
With Pattern		Without Pattern		

TABLE II

PERFORMANCE INDICATORS FOR ALL THE SAMPLES FOR THE ADHERENCE TESTS ON A SOFT ORGANIC TISSUE (CHICKEN). THE COLOUR CODE IS THE SAME USED IN FIGS. 7–10 (RED - SPACED, ORANGE - ADJACENT AND YELLOW - CONTINUOUS SUCTION CUPS)

Sample	Indicator	Sample	Indicator	
(a)	5.6	(b)	4.6	
(c)	6.1	(d)	5.6	Circular
(e)	10.2	(f)	13.4	
(g)	6.3	(h)	7.3	
(i)	7.8	(j)	7.8	Squared
(k)	15.9	(l)	13.4	
With Pattern		Without Pattern		

IV. CONCLUSION

In this letter, the concept of pneumatically attachable flexible rails for MIS surgical applications has been introduced for the first time. In this first design study we have investigated how to optimize the design of the proposed system in order to maximize its adherence to the targeted organs. Future work will investigate on the use of the proposed system with peri-operative surgical imaging probes and the coupling with the da Vinci surgical robot system.

Preliminary ex-vivo tests have been also performed on adult pig kidneys, showing that it is possible to firmly anchor the proposed system by means of vacuum pressure, connect a US-probe paired with the clip-on custom connector and slide it along

suction surface with the same footprint of their non-patterned counterparts, thus offering also a higher friction between the system and the underlying tissue.

The quantitative tests detailed in this section as well as the qualitative tests mentioned at the end of Section II, have also shown how the continuous designs are those more prone to self-reconnect to the target tissue when partially detached, a useful feature for the envisioned application.

the whole length of the rail, without causing the system to detach and without damaging the underlying surface of the tissue.

Further investigation is required about the long-term exposure to vacuum pressure, especially in the case of in-vivo tests on highly vascularized tissue as happens with kidneys. After this preliminary design study of the system, a clinical trial was conducted involving four specialized surgeons (urologists) who were invited to test the proposed system during ex-vivo trials on pig kidneys. During these tests the best performing design for soft tissues, the design (k), has been used.

The results of this study have been presented in a paper named "Autonomous Pick-And-Place of a Novel Robotic Surgery Imaging Rail Using the dVRK Platform*" – C. D'Ettorre, G. Dwyer, A. Stilli, M. Tran, D. Stoyanov, currently under review for ICRA 2019. The team of clinicians involved in this trial among other feedback commented extremely positively on the potential of the PAF rail as organ retractor given the delicate interaction and the firm connection they offer in comparison with the direct use of traditional rigid laparoscopic tools.

The system here presented has been developed for use in RAPN, as this common procedure is among those which can benefit the most of this novel approach, nonetheless its use can be extended to several other procedures (e.g., prostatectomy, partial hepatectomy) and sensing probes (e.g., γ-/β-imaging). Not only the abdominal, but also the pelvic and the thoracic cavities and the organs therein can be targeted. Furthermore, the design of the proposed system allows for ease of customization according to the size of the organ or internal body wall targeted. In this context, future work will also investigate the use of the proposed system in different surgical procedures targeting organs in the aforementioned cavities.

The design of the PAF rails as well as of the custom connector will be also optimized to meet the manufacturing requirements of class III medical devices, exploring the use of bio-compatible 3D printing materials as well as of moulding techniques. Partnerships with healthcare engineering companies will be explored in this context to speed up both the regulatory pathway for clinical trials and the product development itself.

One of the most ambitious long-term of goals of this research is to use the PAF rails as visual references of known shape and size in the field of view of the endoscope, thus allowing more accurate super-imposition of US-reconstructed 3D images of the tumour in augmented reality (AR).

REFERENCES

[1] H. J. Marcus *et al.*, "Trends in the diffusion of robotic surgery: A retrospective observational study," *Int. J. Med. Robot. Comput. Assist. Surg.*, vol. 13, no. 4, 2017, Art. no. e1870.

[2] S. Kaul *et al.*, "Da Vinci-assisted robotic partial nephrectomy: Technique and results at a mean of 15 months of follow-up," *Eur. Urology*, vol. 51, no. 1, pp. 186–192, 2007.

[3] A. J. Wang and S. B. Bhayani, "Robotic partial nephrectomy versus laparoscopic partial nephrectomy for renal cell carcinoma: Single-surgeon analysis of >100 consecutive procedures," *Urology*, vol. 73, no. 2, pp. 306–310, 2009.

[4] C. G. Rogers, A. Singh, A. M. Blatt, W. M. Linehan, and P. A. Pinto, "Robotic partial nephrectomy for complex renal tumors: Surgical technique," *Eur. Urology*, vol. 53, no. 3, pp. 514–523, 2008.

[5] S. B. Bhayani, "Da Vinci robotic partial nephrectomy for renal cell carcinoma: An atlas of the four-arm technique," *J. Robot. Surg.*, vol. 1, no. 4, pp. 279–285, 2008.

[6] L.-M. Su, B. P. Vagvolgyi, R. Agarwal, C. E. Reiley, R. H. Taylor, and G. D. Hager, "Augmented reality during robot-assisted laparoscopic partial nephrectomy: Toward real-time 3D-CT to stereoscopic video registration," *Urology*, vol. 73, no. 4, pp. 896–900, 2009.

[7] W. B. Shingleton and P. E. Sewell Jr., "Percutaneous renal tumor cryoablation with magnetic resonance imaging guidance," *J. Urology*, vol. 165, no. 3, pp. 773–776, 2001.

[8] B. F. Kaczmarek *et al.*, "Robotic ultrasound probe for tumor identification in robotic partial nephrectomy: Initial series and outcomes," *Int. J. Urology*, vol. 20, no. 2, pp. 172–176, 2013.

[9] B. F. Kaczmarek *et al.*, "Comparison of robotic and laparoscopic ultrasound probes for robotic partial nephrectomy," *J. Endourology*, vol. 27, no. 9, pp. 1137–1140, 2013.

[10] N. J. Nickl *et al.*, "Clinical implications of endoscopic ultrasound: The American endosonography club study," *Gastrointestinal Endoscopy*, vol. 44, no. 4, pp. 371–377, 1996.

[11] W. M. Kier and A. M. Smith, "The morphology and mechanics of octopus suckers," *Biol. Bull.*, vol. 178, no. 2, pp. 126–136, 1990.

[12] W. M. Kier and A. M. Smith, "The structure and adhesive mechanism of octopus suckers," *Integrative Comparative Biol.*, vol. 42, no. 6, pp. 1146–1153, 2002.

[13] F. Tramacere, L. Beccai, M. Kuba, A. Gozzi, A. Bifone, and B. Mazzolai, "The morphology and adhesion mechanism of octopus vulgaris suckers," *PLoS One*, vol. 8, no. 6, 2013, Art. no. e65074.

[14] M. Calisti *et al.*, "An octopus-bioinspired solution to movement and manipulation for soft robots," *Bioinspiration Biomimetics*, vol. 6, no. 3, 2011, Art. no. 036002.

[15] S. Sareh *et al.*, "Anchoring like octopus: Biologically inspired soft artificial sucker," *J. Roy. Soc. Interface*, vol. 14, no. 135, vol. 14, no. 135, pp. 1–9, 2017.

[16] Y. Wang *et al.*, "A biorobotic adhesive disc for underwater hitchhiking inspired by the remora suckerfish," *Sci. Robot.*, vol. 2, 2017, Art. no. eaan8072.

[17] T. Tomokazu, S. Kikuchi, M. Suzuki, and S. Aoyagi, "Vacuum gripper imitated octopus sucker-effect of liquid membrane for absorption," in *Proc. IEEE/RSJ Int. Conf. Intell. Robots Syst.*, Hamburg, Germany, 2015, pp. 2929–2936.

[18] S. Ohno, C. Hiroki, and W. Yu, "Design and manipulation of a suction-based micro robot for moving in the abdominal cavity," *Adv. Robot.*, vol. 24, no. 12, pp. 1741–1761, 2010.

[19] N. A. Patronik, M. A. Zenati, and C. N. Riviere, "Preliminary evaluation of a mobile robotic device for navigation and intervention on the beating heart," *Comput. Aided Surg.*, vol. 10, no. 4, pp. 225–232, 2005.

[20] G. Knight, W. D. Fox, and D. R. Schulze, "Cardiac stabilizer device having multiplexed vacuum ports and method of stabilizing a beating heart," U.S. Patent 6 589 166, Jul. 8, 2003.

[21] B. Schena, "Extendable suction surface for bracing medial devices during robotically assisted medical procedures," U.S. Patent 8 377 045, Feb. 19, 2013.

[22] W. Xie, V. Kothari, and B. S. Terry, "A bio-inspired attachment mechanism for long-term adhesion to the small intestine," *Biomed. Microdevices*, vol. 17, no. 4, pp. 1–9, 2015.

[23] H. Kim *et al.*, "Development of a wall-climbing robot using a tracked wheel mechanism," *J. Mech. Sci. Technol.*, vol. 22, no. 8, pp. 1490–1498, 2008.

[24] C. S. Taylor *et al.*, "Surgical instrument for stabilizing the beating heart during coronary artery bypass graft surgery," U.S. Patent 6 346 077, Feb. 12, 2002.

[25] A. D. Ramans, D. J. Rosa, and V. Falk, "Stabilizer for robotic beating-heart surgery," U.S. Patent 6 764 445, Jul. 20, 2004.

[26] A. Roth, *Vacuum Technology*. New York, NY, USA: Elsevier, 2012.